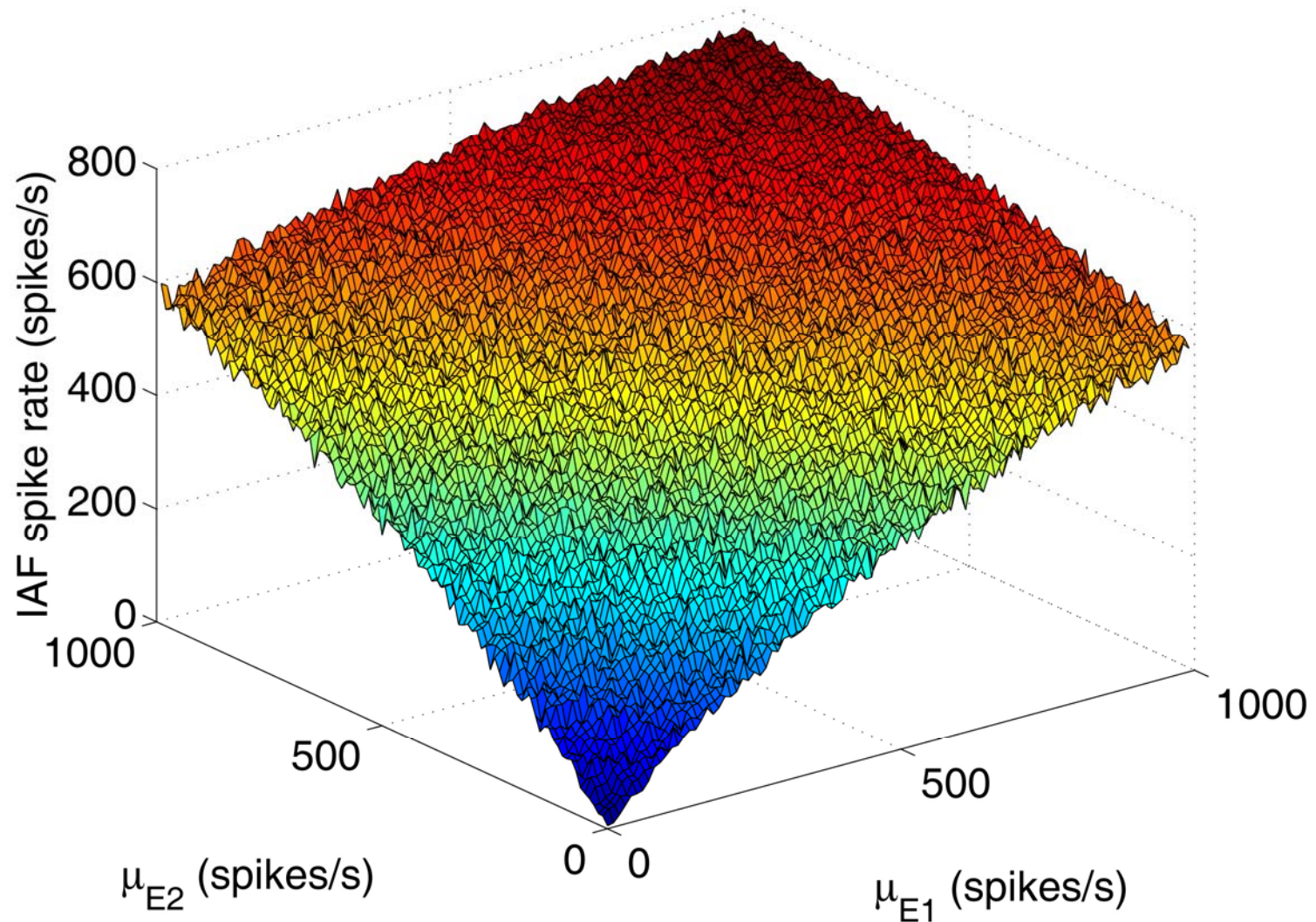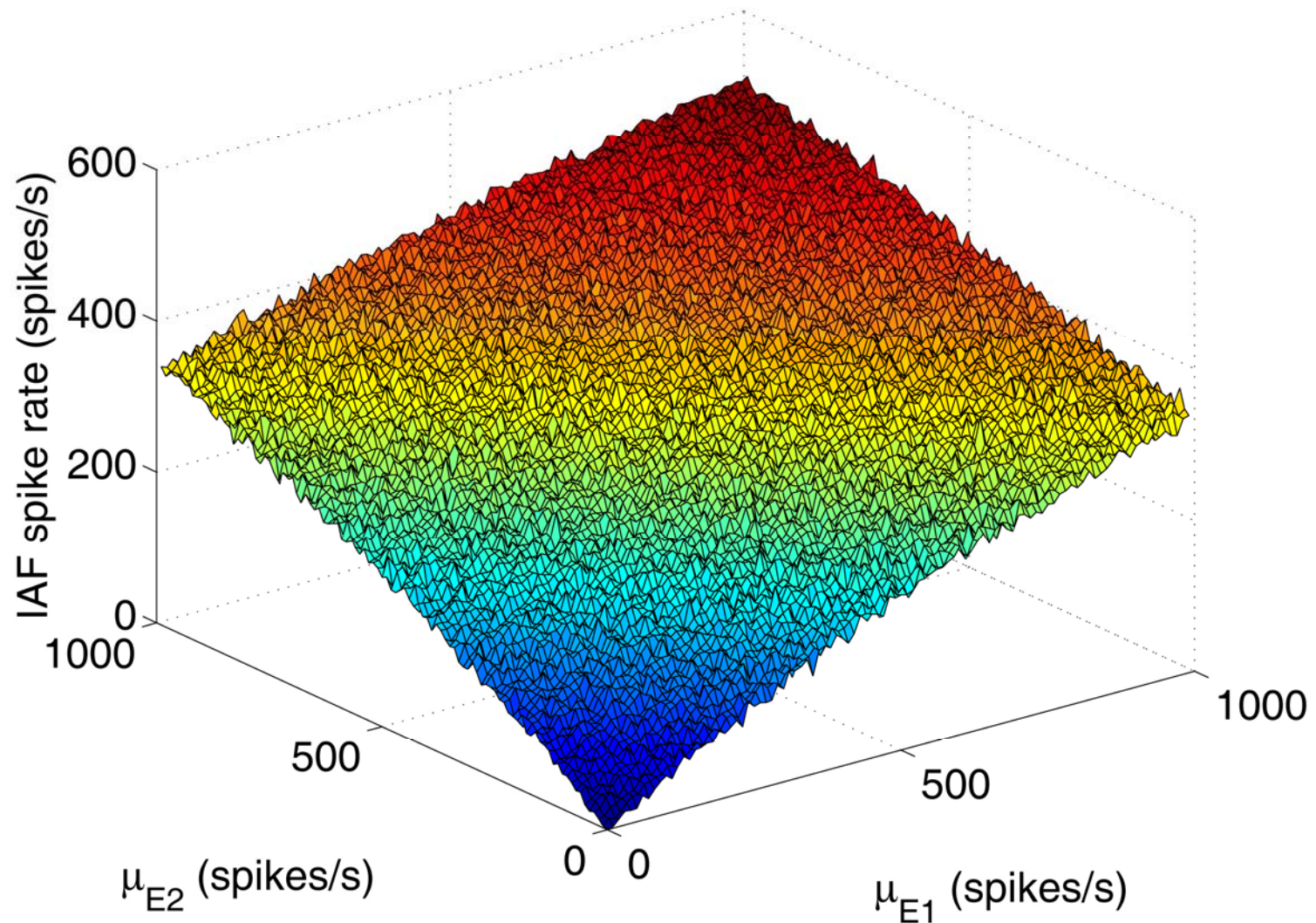# ECE 796:

Models of the Neuron

Slides for Lecture #10
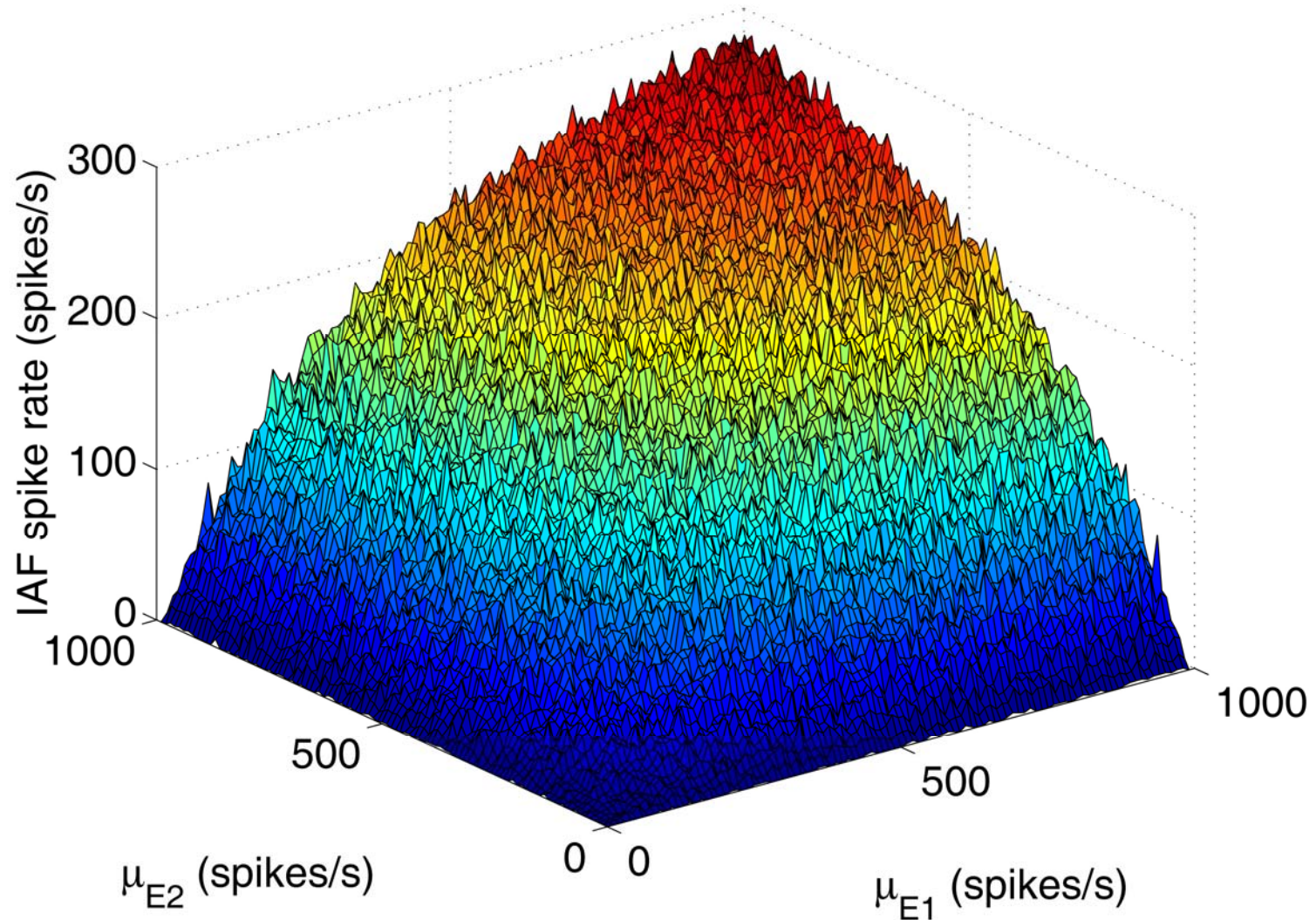
Monday, March 23, 2009

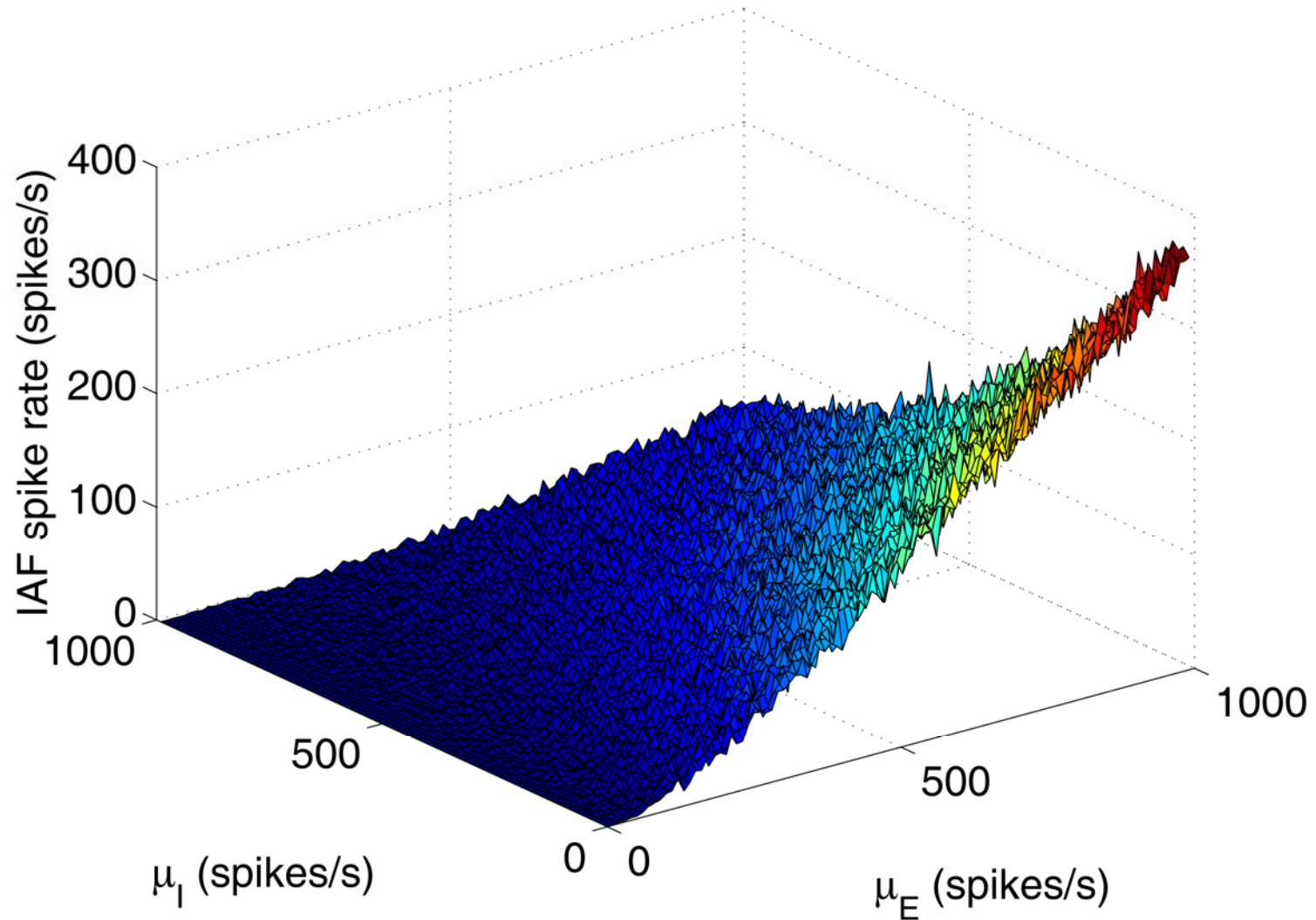# IAF – addition with fast membrane dynamics

IAF – addition with
slow membrane dynamics

IAF – multiplication

IAF – subtraction with hyperpolarizing inhibition
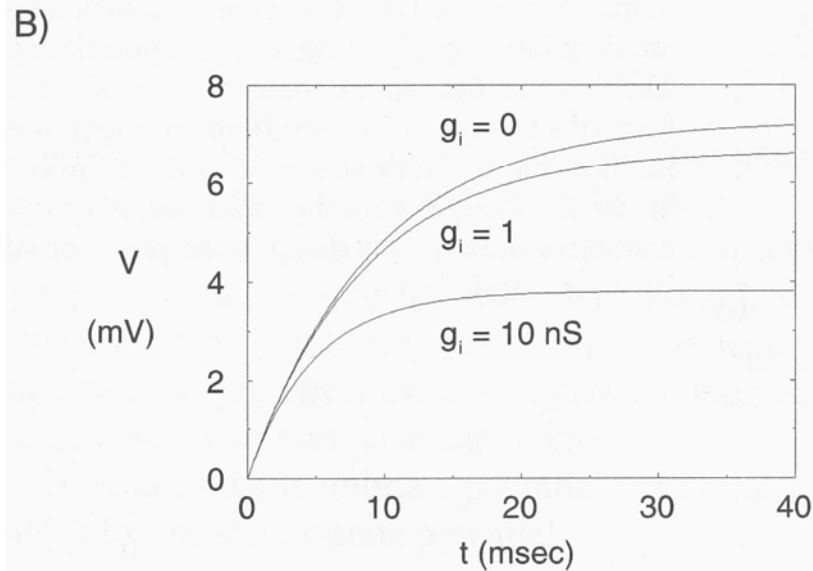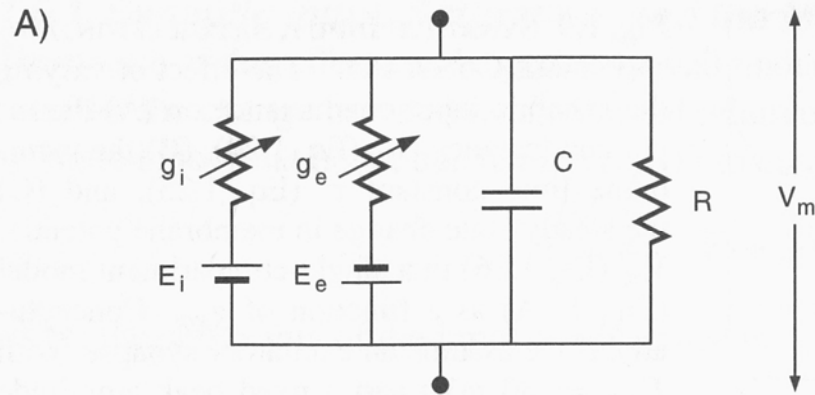
A)

B)

Fig. 1.10 NONLINEAR INTERACTION BETWEEN EXCITATION AND SHUNTING INHIBITION Inhibitory synaptic input of the shunting type, that is, whose reversal potential is close to the cell's resting potential, can implement a form of division. **(A)** This is demonstrated for an RC circuit ($R = 100\,M\Omega$, $C = 100\,pF$) in the presence of both excitation (with battery $E_e = 80\,mV$) and shunting inhibition (with $E_i = 0$). We are here only considering the change in membrane potential relative to V_{rest}. **(B)** Time course of the membrane depolarization in response to a step onset of both excitation (of amplitude $g_e = 1\,nS$) and shunting inhibition (for three values of $g_i = 0$, 1, and 10 nS). One effect of increasing g_i is an almost proportional reduction in EPSP amplitude. A further consequence of increasing the amount of shunting inhibition is to decrease the time constant τ', from its original 10 msec in the absence of any synaptic input to 9 msec in the presence of only excitation to 4.8 msec in the presence of excitation and the 10 times larger shunting inhibition.
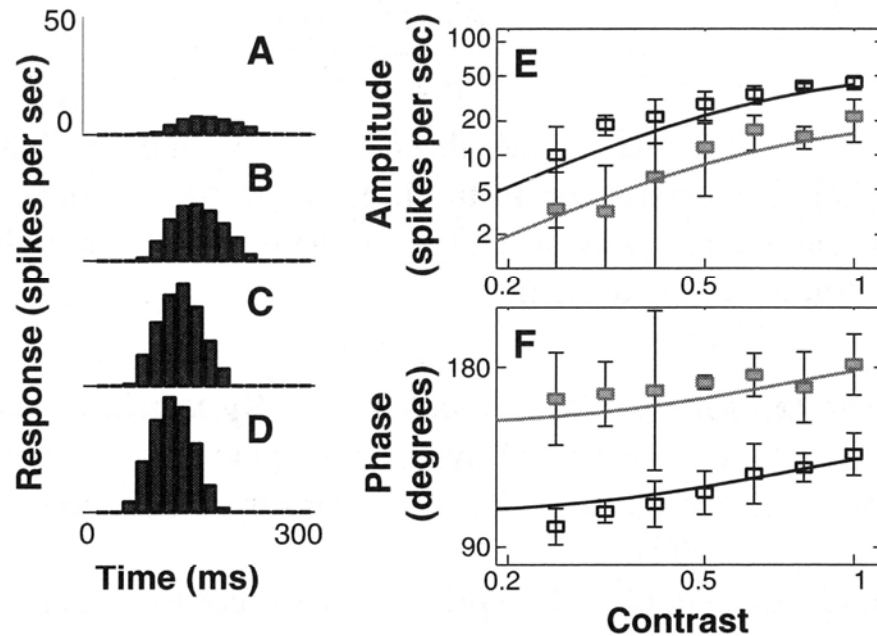
Fig. 1.11 GAIN NORMALIZATION IN NEURONS IN VISUAL CORTEX   Response properties of a simple cell in primary visual cortex of the monkey in response to drifting sinusoidal gratings (Carandini and Heeger, 1994). (**A**) through (**D**) One cycle of the response to gratings of contrast 0.125, 0.25, 0.5, and 1.0. The cell saturates with contrast (doubling the contrast doubles the neuronal response when going from **A** to **B**, but not when going from **C** to **D**) and advances its response (a shift of about 50 msec occurs between **A** and **D**). (**E**) Amplitude and (**F**) Phase of the fundamental Fourier component to sinusoidal gratings drifting at 6 Hz. Shown are the responses of the cell at its preferred orientation (open symbols) and 20° away from the preferred orientation (solid symbols). Error bars represent ±1 standard deviation and the solid lines correspond to the best fit of the model equation that uses shunting inhibition, activated via massive feedback, to carry out this gain normalization. Reprinted by permission from Carandini and Heeger (1994).

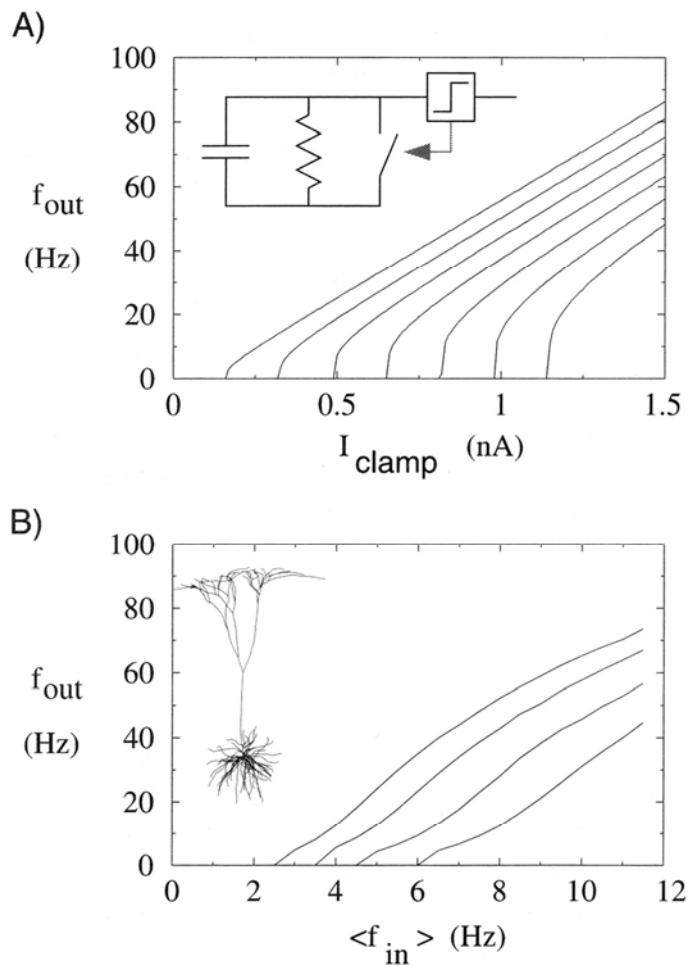# IAF – subtraction with shunting inhibition
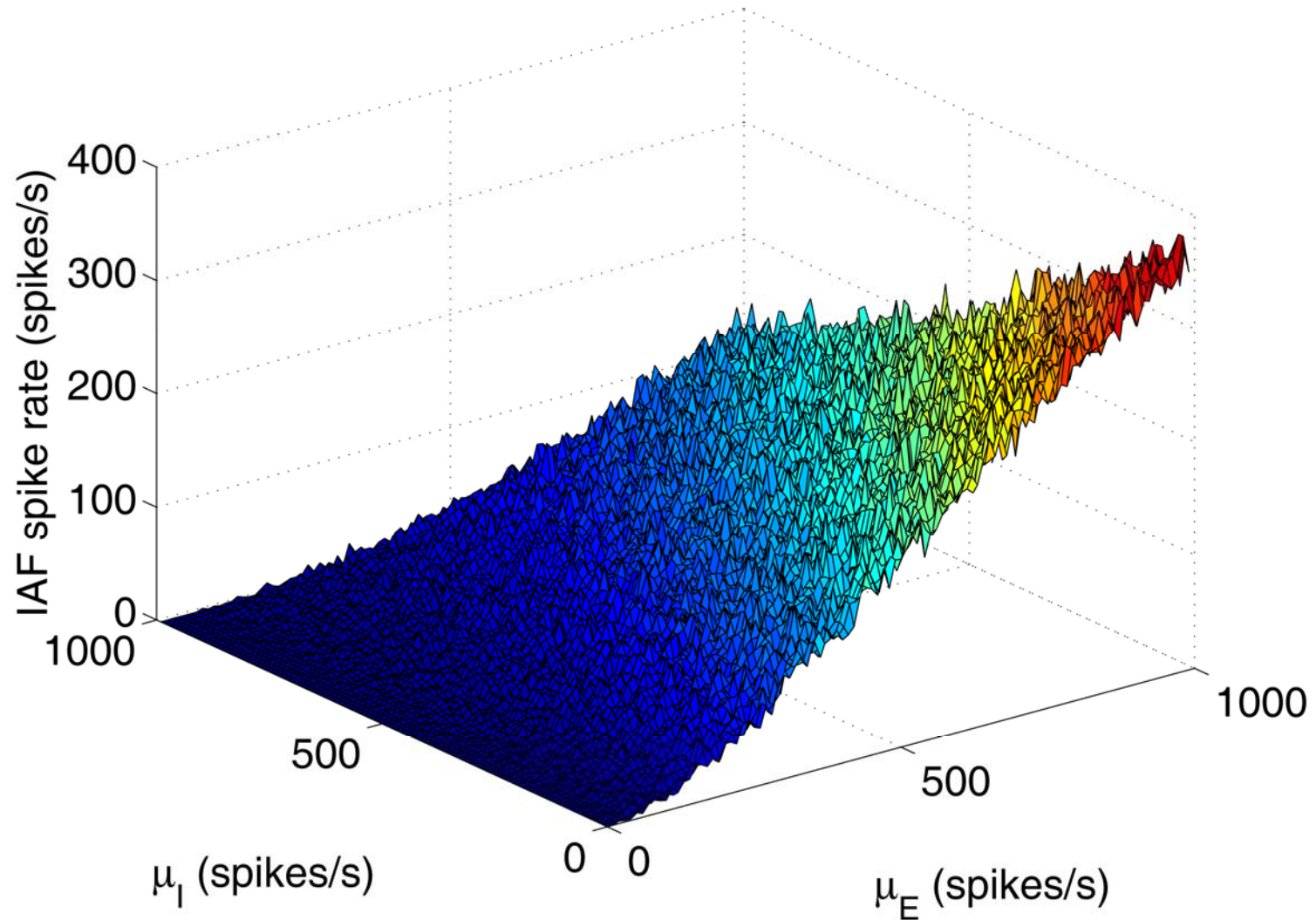
Fig. 18.11 SHUNTING INHIBITION AND SPIKING   Shunting inhibition has a subtractive rather than a divisive effect on firing rates. This is demonstrated in two different single-cell models. **(A)** Discharge curves for a leaky integrate-and-fire unit with different values for the leak conductance $g_{leak} = g_i + 1/R$ (for $R = 62.5 M\Omega$). g_i is the amplitude of the inhibitory conductance change whose reversal potential is equal to the unit's resting potential (here zero). Varying g_{leak} in steps of 10 nS from 10 to 70 nS (from left to right) shifts the curve, rather than changing the slope of the discharge curve. **(B)** The same observation is made in the pyramidal cell model, with $GABA_A$ inhibition around the soma and excitatory voltage-independent input distributed throughout the cell. The fully adapted postsynaptic firing rate is plotted as a function of the average input frequency to the excitatory synapses for four different settings of presynaptic firing rates to the $GABA_A$ synapses (0.5, 2, 4, and 6 Hz, left to right). Reprinted by permission from Holt and Koch (1997).
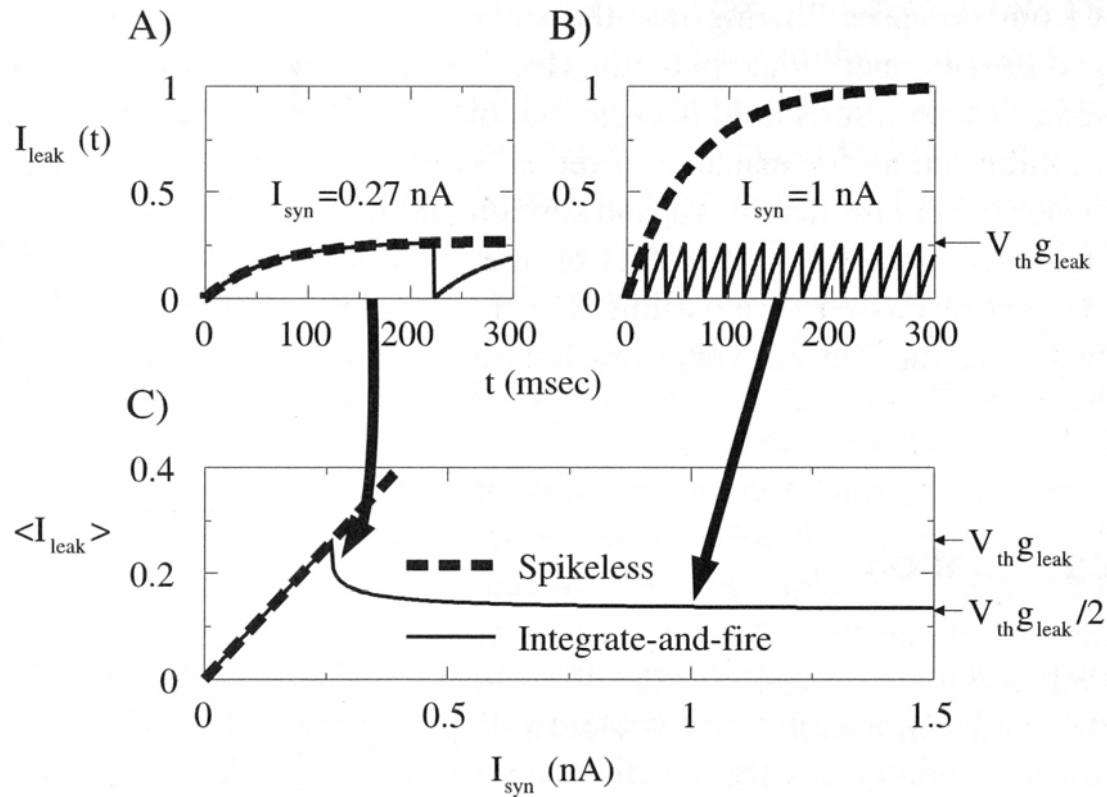
Fig. 18.12 WHY SHUNTING INHIBITION HAS A SUBTRACTIVE EFFECT (A) Time-dependent current across the leak conductance I_{leak} (in nA and equal to $V(t)g_{leak}$) in response to a constant 0.5-nA current injected into a leaky integrate-and-fire unit with (solid line) and without (dashed line) a voltage threshold V_{th}. The sharp drop in I_{leak} occurs when the cell fires, since the voltage is reset. (B) Same for 1-nA current. Note that I_{leak} in the presence of a voltage threshold has a maximum value well below I_{leak} in the absence of a voltage threshold. (C) Time-averaged leak current $\langle I_{leak} \rangle$ (in nanoamperes) as a function of input current, computed from Eqs. 18.24 and 18.25. Below threshold, the spikeless model and the integrate-and-fire model have the same $\langle I_{leak} \rangle$, but above threshold $\langle I_{leak} \rangle$ is reduced considerably. For I_{syn} just greater than threshold, the cell spends most of its time with $V \approx V_{th}$, so $\langle I_{leak} \rangle$ is high. For high I_{syn}, the voltage increases approximately linearly with time and V has a sawtooth waveform, as shown in **B**. This means that $\langle I_{leak} \rangle = (\max I_{leak})/2 = V_{th}g_{leak}/2$. Reprinted by permission from Holt and Koch (1997).
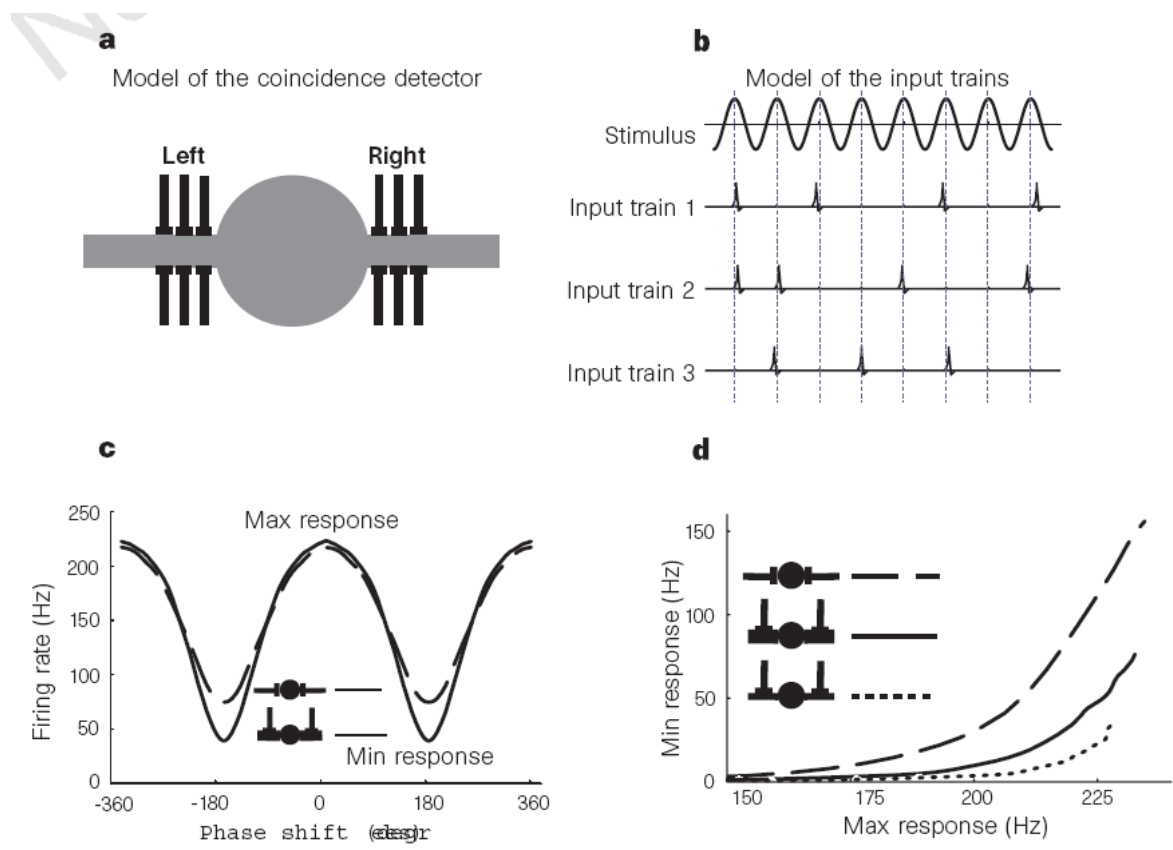
Figure 2 A bipolar-neuron model for coincidence detection. **a**, The bipolar-neuron model consists of a soma (centre) and two cylindrical dendrites (see Methods). **b**, Inputs resembled *in vivo* inputs (see Methods). **c**, Model ITD curves for a 500-Hz stimulus showed an improvement in ITD coding when dendrites were added (0.2-λ thick (4 μm) passive dendrites). The contrast between the maximum spike rate (0° delay) and the minimum spike rate (180° delay) was larger when the inputs were segregated on the dendrites (solid line; USC = 0.022 μS), compared with the point-neuron model (dashed line; USC = 0.01 μS). **d**, Parametric plot of different input configurations shows the relationship between maximum and minimum spike rates as the USC changes. Dashed line, inputs on soma, USC range 0.007–0.011 μS; solid line inputs on thick (4 μm diameter) dendrites, USC range 0.013–0.024 μS; dotted line, inputs on thin (2 μm diameter) dendrites, USC range 0.014–0.026 μS. Dendritic USCs were made larger than somatic USCs to provide similar maximum responses.
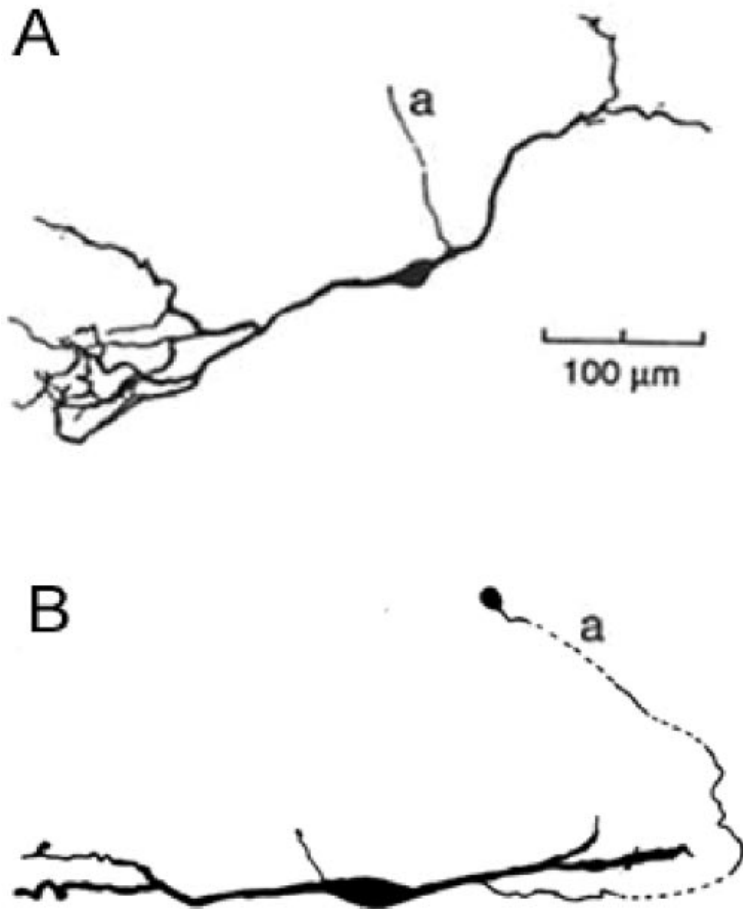
(from Agmon-Snir et al., *Science* 1998)

Figure 1. The asymmetrical cell structure with an axon (a) emerging from the ipsilaterally innervated dendrite. *A*, A cell from a guinea pig MSO [reproduced from Smith (1995) with permission]. *B*, A cell from a gerbil MSO (Golding, unpublished observation) (scale bar not shown). Both cells have an axon emerging from the ipsilaterally innervated dendrite.
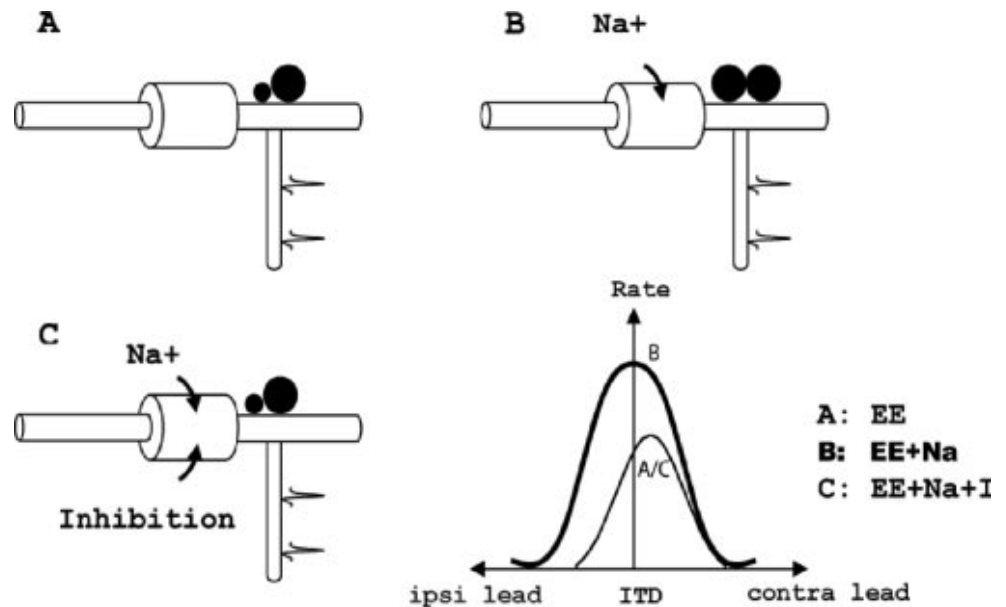
Figure 4. Illustration of the mechanisms involved in the bipolar model. Three soma membrane conditions that were studied were a simple RC circuit (EE) (*A*), the RC circuit with active sodium channels (EE+Na) (*B*), and the RC circuit with active sodium channels and with inhibitory synapses (EE+Na+I) (*C*). Zero ITD corresponds to zero arrival delay between the two excitatory inputs. ipsi, Ipsilateral; contra, contralateral.

(from Zhou et al., *J. Neurosci.* 2005)